Chinese Physics B

中国物理学会
Chinese Physical Society

PAPER

Gate tunable Rashba spin-orbit coupling at $CaZrO_3/SrTiO_3$ heterointerface

To cite this article: Wei-Min Jiang *et al* 2022 *Chinese Phys. B* **31** 066801

View the article online for updates and enhancements.

You may also like

- Synthesis and scintillation properties of Ce-doped $CaZrO_3$ single crystals
Hiroyuki Fukushima, Daisuke Nakauchi, Masanori Koshimizu et al.

- Effects of Ti doping on scintillation properties of $CaZrO_3$ single crystals
Hiroyuki Fukushima, Daisuke Nakauchi, Takumi Kato et al.

- Characterization of $CaZrO_3$ Coating Layer Formed on YSZ Plate for SOM Anode in $CaCl_2$-CaF_2-CaO Electrolyte
Wan-Bae Kim, Hayk Nersisyan, Suk-Cheol Kwon et al.

This content was downloaded from IP address 159.226.165.22 on 14/02/2023 at 01:19

Chin. Phys. B **31**, 066801 (2022)

Gate tunable Rashba spin–orbit coupling at $CaZrO_3/SrTiO_3$ heterointerface

Wei-Min Jiang(姜伟民)[1,†], Qiang Zhao(赵强)[1,†], Jing-Zhuo Ling(凌靖卓)[1], Ting-Na Shao(邵婷娜)[1], Zi-Tao Zhang(张子涛)[1], Ming-Rui Liu(刘明睿)[2], Chun-Li Yao(姚春丽)[1], Yu-Jie Qiao(乔宇杰)[1], Mei-Hui Chen(陈美慧)[1], Xing-Yu Chen(陈星宇)[1], Rui-Fen Dou(窦瑞芬)[1,‡], Chang-Min Xiong(熊昌民)[1,§], and Jia-Cai Nie(聂家财)[1,¶]

[1] *Department of Physics, Beijing Normal University, Beijing* 100875, *China*

[2] *State Key Laboratory of Luminescence and Applications, Changchun Institute of Optics, Fine Mechanics and Physics, Chinese Academy of Sciences, Changchun* 130033, *China*

(Received 15 December 2021; revised manuscript received 28 January 2022; accepted manuscript online 10 February 2022)

High mobility quasi two-dimensional electron gas (2DEG) found at the $CaZrO_3/SrTiO_3$ nonpolar heterointerface is attractive and provides a platform for the development of functional devices and nanoelectronics. Here we report that the carrier density and mobility at low temperature can be tuned by gate voltage at the $CaZrO_3/SrTiO_3$ interface. Furthermore, the magnitude of Rashba spin–orbit interaction can be modulated and increases with the gate voltage. Remarkably, the diffusion constant and the spin–orbit relaxation time can be strongly tuned by gate voltage. The diffusion constant increases by a factor of ~ 19.98 and the relaxation time is reduced by a factor of over three orders of magnitude while the gate voltage is swept from -50 V to 100 V. These findings not only lay a foundation for further understanding the underlying mechanism of Rashba spin–orbit coupling, but also have great significance in developing various oxide functional devices.

Keywords: $CaZrO_3/SrTiO_3$, 2DEG, Rashba spin–orbit coupling, gate voltage

PACS: 68.47.Gh, 73.20.–r, 81.15.Fg

DOI: 10.1088/1674-1056/ac5396

1. Introduction

Owing to the rapid development of film technology, a large amount of oxide heterointerfaces among transition metal oxides (TMOs) have been fabricated intensively, exhibiting a lot of intriguing physical functionalities because of their unique electronic structure and properties.[1–10] One typical breakthrough was that the interface between two ABO_3 type perovskite insulators, *e.g.*, $LaAlO_3$ and $SrTiO_3$ (LAO/STO), hosts a high-mobility two-dimensional electron gas (2DEG).[11] The conductive interface possesses quantities of fascinating properties such as ferromagnetism,[12–14] superconductivity,[15,16] and strong Rashba spin–orbit coupling (Rashba-SOC),[17] which results from the interfacial breaking of inversion symmetry.

Apart from the LAO/STO interface, 2DEGs have also been found in other STO-based systems.[18–24] In 2015, Chen *et al.* created a newly nonpolar interface in 3d strong correlated systems, $CaZrO_3/SrTiO_3$ (CZO/STO). The critical thickness of CZO is 6 unit cell for the occurrence of interface conduction and it is much attractive via its high electron mobility more than 6×10^4 $cm^2/(V\cdot s)$ at low temperature, almost three times of the mobility of 2DEG at the LAO/STO interface.[25] Meanwhile, Niu *et al.* tuned the CZO/STO interface by using external ionic liquids (ILs) gating according to the electrolyte gate mechanism.[26] Besides, compared to the LAO/STO interface, the CZO/STO interface has a better lattice match and nonpolar property, which may have critical reference not only for the investigation of conductive mechanism but also for the study of diversified novel physical properties, such as Rashba-SOC, in CZO/STO system.

So far, however, the effect of the external gate voltage (V_G) on the transport properties at the CZO/STO interface has not yet been systematically studied. In our work, the effects of V_G on the 2DEG transport properties at the CZO/STO interface, including Rashba-SOC, are studied. Our results show that tunable Rashba-SOC is susceptible to the external V_G.

2. Experimental details

CZO films with 22-unit-cells (~ 8.8 nm) were grown on (001)-oriented TiO_2-terminated STO single-crystal substrates (5 mm×5 mm×0.5 mm with miscut less than 0.2°) by pulsed laser deposition (PLD) at 600 °C in an oxygen atmosphere of $\sim 10^{-4}$ mbar (1 bar $=10^5$ Pa). During deposition, the repetition rate of laser pulse was 1 Hz and the fluence was 1.5 J/cm^2 (KrF laser, $\lambda = 248$ nm). After deposition, the sample was cooled down to room temperature with a rate of 15 °C/min

[†] These authors contributed equally to this work.
[‡] Corresponding author. E-mail: ruifendou@bnu.edu.cn
[§] Corresponding author. E-mail: cmxiong@bnu.edu.cn
[¶] Corresponding author. E-mail: jcnie@bnu.edu.cn
© 2022 Chinese Physical Society and IOP Publishing Ltd
http://iopscience.iop.org/cpb http://cpb.iphy.ac.cn

without changing the oxygen pressure. The target-substrate distance was fixed at 5.6 cm.

The electrode contacts were made using Van der Pauw method by ultrasonic wire bonding (Al wire of 20 μm in diameter). All the transport properties were performed by a physical property measurement system (PPMS, Quantum Design) in the temperature range from 2 K to 300 K. The applied current for resistance measurements was 10 μA. The V_G was applied to a back gate on the side of STO while the 2DEG was grounded. The leakage current was lower than 10 nA.

3. Results and discussion

To bring out the potential aspects of our 2DEG, a systematic investigation on gating effect is desirable. Figure 1(a) shows the schematic device structure. Figure 1(b) shows the sheet resistance (R_s) for the sample under different gate voltages at 2 K, R_s decreases from $\sim$ 19579.35 $\Omega/\square$ to $\sim$ 979.29 $\Omega/\square$ as V_G sweeps from -50 V to 100 V, reduced by a factor of 20. Figure 1(c) shows the Hall resistance measured at 2 K under different gate voltages from 0 to 9 T. All R_{xy}–B curves are well linear, signifying that there is only one species of charge carriers in the 2DEG. The collapse of the R_{xy}–B curve with the increase of V_G identifies the increase of the carrier density (n_s). According to the formula, $n_s = -1/R_H e$, (e is the charge of an electron), n_s is obtained. Actually, the tuning ability can be estimated as $\delta n_{2D} = \varepsilon_0 \varepsilon_r V_G/t$, where ε_0 is the vacuum permittivity, ε_r and t are the dielectric constant and the thickness of a dielectric material respectively.[27] Therefore, the required gate voltage is independent of CZO thickness. Figure 1(d) illustrates the carrier density as a function of the gate voltage. With the V_G ranging from -50 V to 100 V, the n_s at 2 K increases from $\sim 1.17 \times 10^{13}$ cm^{-2} to $\sim 1.80 \times 10^{13}$ cm^{-2}. Based on the data in Figs. 1(b) and 1(d), Hall mobility (μ) can be worked out. As charge carriers are accumulated, as shown in Fig. 1(e), the gate voltage tunes the mobility from $\sim$ 27.29 cm^2/(V·s) to $\sim$ 354.56 cm^2/(V·s), increased by a factor of 13.

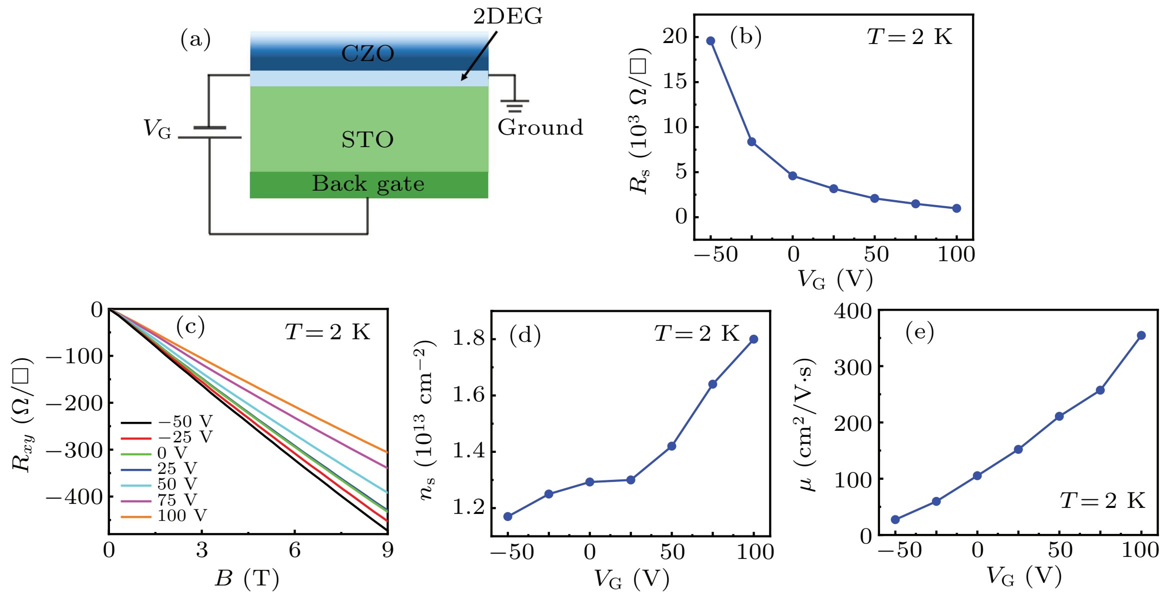

Fig. 1. (a) A schematic device structure. (b) Sheet resistance as a function of the gate voltages from -50 V to 100 V at a fixed temperature of 2 K. (c) Gating effect on Hall resistance measured at 2 K. (d) and (e) Carrier density and Hall mobility as functions of the gate voltages, obtained at 2 K.

Another problem to be addressed is the gating effect of quantum interference, which is a unique characteristic of 2DEG. After gating 2DEG to the preset state, we measured the sheet resistance in the perpendicular magnetic field. Figure 2(a) shows the magnetoresistance (MR) at a fixed temperature of 2 K, defined by $MR = [R_s(B) - R_s(B=0)]/R_s(B=0)$, as a function of magnetic field ($B \perp$interface) by applying various gate voltages. Two features can be identified from the data in Fig. 2(a). The first one is the occurrence of a sharp minimum at $B = 0$ in all MR–B curves, which is a fingerprint of weak antilocalization owing to the Rashba-SOC. When the applied magnetic field is high enough, MR grows smoothly, which is the classical orbital effect of the magnetic field. Secondly, for $V_G = 0$ and negative values, MR first grows and then decreases, *i.e.* the weak antilocalization and weak localization become weakened, respectively.

It can be obviously seen in Fig. 2(b) that $\Delta\sigma/\sigma_0$ changes significantly under different gate voltages. $\Delta\sigma/\sigma_0$ is defined by $\Delta\sigma(B)/\sigma_0 = [\sigma(B) - \sigma(B=0)]/(e^2/\pi h)$, where $\sigma(B)$ is the magnetoconductance at a magnetic field, and $\sigma_0 = e^2/\pi h$ is the quantum conductance. In order to better understand the Rashba-SOC of the 2DEG at the CZO/STO interface, we carried out the detailed analysis of the magnetoconductance, which is a typical characteristic of weak antilocalization due to Rashba-like SOC. The first order correction to the conductance $\Delta\sigma$ is based on the Maekawa–Fukuyama (MF) equation

while ignoring the effect of Zeeman splitting,[28,29]

$$
\begin{aligned}
\frac{\Delta\sigma(B)}{\sigma_0} = & -\psi\left(\frac{1}{2}+\frac{B_{\rm el}}{B}\right)+\frac{3}{2}\psi\left(\frac{1}{2}+\frac{B_{\rm in}+B_{\rm so}}{B}\right) \\
& -\frac{1}{2}\psi\left(\frac{1}{2}+\frac{B_{\rm in}}{B}\right) \\
& -\left[\ln\left(\frac{B_{\rm in}+B_{\rm so}}{B_{\rm el}}\right)+\frac{1}{2}\ln\left(\frac{B_{\rm in}+B_{\rm so}}{B_{\rm in}}\right)\right] \\
& -A_{\rm k}\frac{\sigma(0)}{\sigma_0}\frac{B^2}{1+CB^2}.
\end{aligned} \tag{1}
$$

In Eq. (1), $\psi(x)$ is digamma function described as $\psi(x) = \ln(x)+\psi(1/2+1/x)$. $B_{\rm el}$, $B_{\rm in}$, $B_{\rm so}$ represent the effective fields related with elastic scattering time ($\tau_{\rm el}$), inelastic scattering time ($\tau_{\rm in}$) and spin–orbit relaxation time ($\tau_{\rm so}$), by the expressions $B_n = \hbar/(4eD\tau_n)$, n = el, in, and so, respectively. The last term is the Kohler term and gives a description of orbital *MR*. $D = v_{\rm F}^2\tau_{\rm el}/2$ is the electronic diffusion constant in 2D systems, where $\tau_{\rm el} = m^*\mu/e$, m^* is the effective electron mass, $v_{\rm F} = \hbar k_{\rm F}/m^*$ is the Fermi velocity, $k_{\rm F} = (2\pi n_{\rm s})^{1/2}$ is the electron wave vector at Fermi energy, $n_{\rm s}$ is the carrier density of 2DEG. As reported by angle-resolved photoemission spectroscopy,[30] the light and heavy masses was assigned to be $m_{\rm l} = 0.7m_{\rm e}$ and $m_{\rm h} = 15m_{\rm e}$ ($m_{\rm e}$ is the free-electron mass) for the *dxy* and *dxz*/*yz* subbands, respectively. Here, we take $m^* = (m_{\rm l}\cdot m_{\rm h})^{1/2} \approx 3.2m_{\rm e}$, as Joshua *et al.*[31] did in the treatment for the combined density of states of 2DEG by using the geometric mean of the effective masses. Thus, the diffusion constant can be derived as $D = \pi\hbar^2 n_{\rm s}\mu/m_{\rm e}^*$. D as a function of $V_{\rm G}$ is plotted in Fig. 2(c).

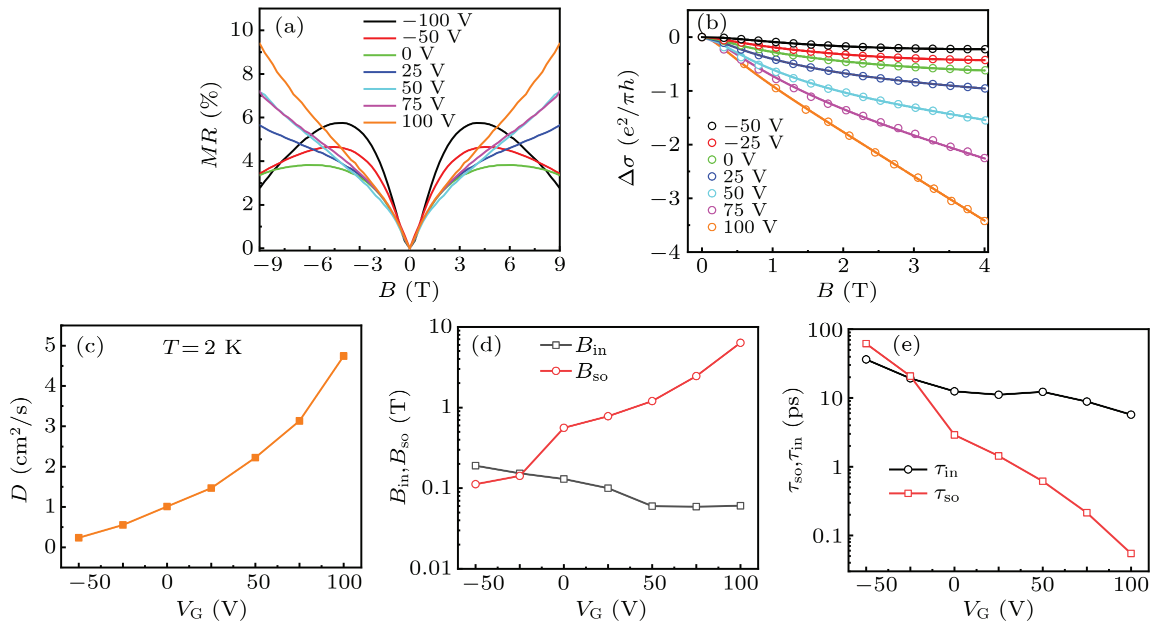

Fig. 2. (a) Magnetoresistance as a function of the perpendicular magnetic field, measured under different gate voltages at a fixed temperature of 2 K. (b) $\Delta\sigma/\sigma_0$ as a function of B ($B\perp$interface) at various different voltages at $T = 2$ K. The solid curves are fitting to Eq. (1). (c) The gate tunable diffusion constant D estimated at 2 K. Panels (d) and (e) show $B_{\rm in}$, $B_{\rm so}$, and $\tau_{\rm in}$, $\tau_{\rm so}$ as a function of $V_{\rm G}$ between −50 V and 100 V, respectively. $B_{\rm in}$, $B_{\rm so}$ are extracted from the fitting curves of the original data.

According to the results of the solid fitting curves in Fig. 2(b), parameters ($B_{\rm el}$, $B_{\rm in}$, $B_{\rm so}$) were obtained from the experimental results for the range of gate voltages from −50 V to 100 V. As shown in Fig. 2(d), $B_{\rm so}$ and $B_{\rm in}$ are well tuned by $V_{\rm G}$. $B_{\rm so}$ is the magnetic field related to the Rashba-SOC and it reflects on the SOC strength of 2DEG at CZO/STO interface. With the $V_{\rm G}$ increases, $B_{\rm so}$ increases from 0.112 T to 6.35 T. In other words, the strength of Rashba-SOC becomes stronger. $B_{\rm in}$ decreases from 0.19 T to 0.0605 T. The values of $B_{\rm so}$ are in the same range as the ones reported previously for other STO-based 2DEGs.[32–35] For negative gate voltages, $B_{\rm in}$ is larger than $B_{\rm so}$ while at $V_{\rm G} \geq 0$ V, $B_{\rm so}$ is larger than $B_{\rm in}$ and increases monotonously with $V_{\rm G}$.

Similarly, the data of $\tau_{\rm in}$ and $\tau_{\rm so}$ with $V_{\rm G}$ are also extracted on the basis of the fitting curves in Fig. 2(e). With the $V_{\rm G}$ increases, $\tau_{\rm in}$ ranges from 36.41 ps to 5.72 ps, $\tau_{\rm so}$ ranges from 61.76 ps to 0.054 ps, reduced by a factor of over three orders of magnitude. Rashba-SOC is dominant in this system. Furthermore, with $V_{\rm G}$ increases from −50 V to 100 V, the diffusion coefficient D increases by 19.98 times, while D of the LAO/STO interface 2DEG changes by only 2.5 times in the same gate voltage range.[32] Therefore, the effective regulation on $\tau_{\rm so}$ we observed results not only from the strong dependence of $B_{\rm so}$ on the gate voltage, but also from the strong dependence of D on the gate voltage.

Owing to the interfacial breaking of inversion symmetry, there is a potential gradient at the surface and interface, and electron SOC leads to band splitting, resulting in spin-momentum locking and spin-chirality opposite band structure (*i.e.* Rashba-SOC effect).[36] Rashba-SOC always exists in 2D

systems such as LAO/STO,[11] CZO/STO,[25] $LaVO_3$/STO,[9] and even amorphous LAO/STO, *etc.*[37,38] Its effect is expressed by the Bychkov–Rashba term $H_R = \alpha_R (k \times \hat{x}) \cdot \sigma$,[39] where σ are Pauli matrices, k is the wave vector, x is a unit vector along the electric filed direction, and α_R is the Rashba parameter which measures the strength of the Rashba-SOC. Vaz *et al.* determined α_R from the response of bilinear magnetoresistance in 2DEG at the LAO/STO interface.[40] They derived the dependence between V_G and α_R, and showed that α_R increases monotonically with V_G and reaches maximum at 120 V.

At the CZO/STO heterointerface, we have demonstrated a gate-tunable Rashba-SOC (see Fig. 2(d)), which originates from the interfacial breaking of inversion symmetry. In fact, as shown in Fig. 3(a), the spin relaxation time τ_{so} is proportional to the inverse of the elastic scattering time (τ_{el}^{-1}) over the gate voltage range from -50 V to 100 V, a clear signature of the D'Yakonov–Perel (DP) mechanism characteristic of the Rashba spin–orbit interaction.[41] Based on the DP mechanism, according to the formula, $\alpha_R = (e\hbar^3 B_{so})^{1/2}/m^*$, we can obtain the α_R value with B_{so}, and the obtained α_R value increases from 0.31 meV·nm to 2.33 meV·nm with increase of V_G (see Fig. 3(b)). Therefore, by applying different V_G, the strength of 2DEG Rashba-SOC can be efficiently controlled.

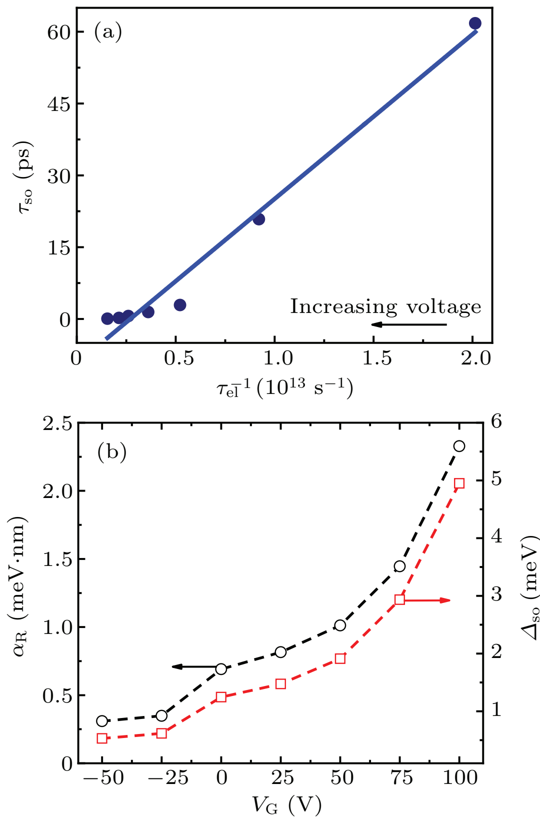

Fig. 3. (a) The dependence of τ_{so} and τ_e^{-1} under different voltages. (b) Left axis, black circles: Rashba parameter α_R under different gate voltages. Right axis, red squares: the Rashba spin-splitting Δ_{so} under different gate voltages.

Furthermore, the corresponding Rashba spin splitting energy $\Delta_{so} = 2k_F\alpha_R$ (note that k_F is related to n_s, which is determined by Hall measurements, see the section below) is also determined, which ranges from 0.53 meV to 4.95 meV (Fig. 3(b)). As can be seen clearly in Fig. 3(b), the strength of Rashba-SOC at CZO/STO interface could be enhanced when applying positive V_G and becomes weakened when applying negative V_G. In a word, compared with the LAO/STO interface,[32] tunable Rashba spin–orbit coupling shows the similar gate dependence at the CZO/STO interface.

4. Conclusion

In summary, we demonstrate that Rashba-SOC of 2DEG at the nonpolar CZO/STO interface are well tuned by external V_G. B_{so} increases from 0.112 T to 6.35 T with the increase of V_G from -50 V to 100 V. Moreover, the mobility also increases from ~ 27.29 cm^2/(V·s) to ~ 354.56 cm^2/(V·s). More importantly, D increases by a factor of ~ 19.98 and τ_{so} can be strongly tuned which is reduced by a factor of over three orders of magnitude. Our results facilitate the development of more complex oxides heterointerfaces and provide new opportunities for designing electronic applications in traditional semiconductor devices.

Acknowledgement

Project supported by the National Natural Science Foundation of China (Grants Nos. 92065110, 11974048, and 12074334).

References

[1] Wang Y X 2009 *Chin. Phys. Lett.* **26** 016801
[2] Chen X L, Chen L, Zhou Z X and Zhao Y 2018 *Acta Phys. Sin.* **67** 118401 (in Chinese)
[3] Panahi N, Hosseinnejad M T, Shirazi M and Ghoranneviss M 2016 *Chin. Phys. Lett.* **33** 066802
[4] Shen S C, Hong Y P, Li C J, Xue H X, Wang X X and Nie J C 2016 *Chin. Phys. B* **25** 076802
[5] Chakhalian J, Freeland J W, Millis A J, Panagopoulos C and Rondinelli J M 2014 *Rev. Mod. Phys.* **86** 1189
[6] Wei S Y, Wang Z G and Yang Z X 2007 *Chin. Phys. Lett.* **24** 800
[7] Moetakef P, Williams J R, Ouellette D G, Kajdos A P, GoldhaberGordon D, Allen S J and Stemmer S 2012 *Phys. Rev. X* **2** 021014
[8] Wang F N, Li J C, Zhang X M, Liu H Z, Liu J, Wang C L, Zhao M L, Su W B and Mei L M 2017 *Chin. Phys. B* **26** 037101
[9] Wang F N, Li J C, Li Y, Zhang X M, Wang X J, Chen Y F, Liu J, Wang C L, Zhao M L and Mei L M 2019 *Chin. Phys. B* **28** 047101
[10] Moetakef P, Cain T A, Ouellette D G, Zhang J Y, Klenov D O, Janotti A, Van de Walle C G, Rajan S, Allen S J and Stemmer S 2011 *Appl. Phys. Lett.* **99** 232116
[11] Ohtomo A and Hwang H Y 2004 *Nature* **427** 423
[12] Dikin D A, Mehta M, Bark C W, Folkman C M, Eom C B and Chandrasekhar V 2011 *Phys. Rev. Lett.* **107** 056802
[13] Bert J A, Kalisky B, Bell C, Kim M, Hikita Y, Hwang H Y and Moler K A 2011 *Nat. Phys.* **7** 767
[14] Reyren N, Gariglio S, Caviglia A D, Jaccard D, Schneider T and Triscone J M 2009 *Appl. Phys. Lett.* **94** 112506
[15] Reyren N, Thiel S, Caviglia A D, Kourkoutis L F, Hammerl G, Richter C, Schneider C W, Kopp T, Rüetschi A S, Jaccard D, Gabay M, Muller D A, Triscone J M and Mannhart J 2007 *Science* **317** 1196
[16] Yin C H, Seiler P, Tang L M K, Leermakers I, Lebedev N, Zeitler U and Aarts J 2020 *Phys. Rev. B* **101** 245114

[17] Gunkel F, Skaja K, Shkabko A, Dittmann R, Hoffmann-Eifert S and Waser R 2013 *Appl. Phys. Lett.* **102** 071601
[18] Chen Y Z, Bovet N, Kasama T, Gao W W, Yazdi S, Ma C, Pryds N and Linderoth S 2014 *Adv. Mater.* **26** 1462
[19] Chen Y Z, Bovet N, Trier F, Christensen D V, Qu F M, Andersen N H, Kasama T, Zhang W, Giraud R, Dufouleur J, Jespersen T S, Sun J R, Smith A, Nygard J, Lu L, Buechner B, Shen B G, Linderoth S and Pryds N A 2013 *Nat. Commun.* **4** 1371
[20] Perna P, Maccariello D, Radovic M, Scotti di Uccio U, Pallecchi I, Codda M, Marré D, Cantoni C, Gazquez J, Varela M, Pennycook S J and Miletto Granozio F 2010 *Appl. Phys. Lett.* **97** 152111
[21] Shibuya K, Ohnishi T, Lippmaa M and Oshima M 2007 *Appl. Phys. Lett.* **91** 232106
[22] Lee S W, Liu Y, Heo J and Gordon R G 2012 *Nano Lett.* **12** 4775
[23] Kim J S, Seo S S A, Chisholm M F, Kremer R K, Habermeier H U, Keimer B and Lee H N 2010 *Phys. Rev. B* **82** 201407
[24] Li. D F, Wang Y and Dai J Y 2011 *Appl. Phys. Lett.* **98** 122108
[25] Chen Y, Trier F, Kasama T, Christensen D V, Bovet N, Balogh Z I, Li H, Thyden K T S, Zhang W, Yazdi S, Norby P, Pryds N and Linderoth S 2015 *Nano Lett.* **15** 1849
[26] Niu W, Chen Y D, Gan Y L, Zhang Y, Zhang X Q, Yuan X, Cao Z, Liu W Q, Xu Y B, Zhang R, Pryds N, Chen Y Z, Pu Y and Wang X F 2019 *Appl. Phys. Lett.* **115** 061601
[27] Chen Z, Liu Y, Zhang H, Liu Z R, Tian H, Sun Y Q, Zhang M, Zhou Y, Sun J R and Xie Y W 2021 *Science* **372** 721
[28] Hurand S, Jouan A, Feuillet-Palma C, Singh G, Biscaras J, Lesne E, Reyren N, Barthélémy A, Bibes M, Villegas J E, Ulysse C, Lafosse X, Pannetier-Lecoeur M, Caprara S, Grilli M, Lesueur J and Bergeal N 2015 *Sci. Rep.* **5** 12751
[29] Singh G, Jouan A, Hurand S, Feuillet-Palma C, Kumar P, Dogra A, Budhani R, Lesueur J and Bergeal N 2017 *Phys. Rev. B* **96** 024509
[30] Santander-Syro A F, Copie O, Kondo T, Fortuna F, Pailhés S, Weht R, Qiu X G, Bertran F, Nicolaou A, Taleb-Ibrahimi A, Le Févre P, Herranz G, Bibes M, Reyren N, Apertet Y, Lecoeur P, Barthélémy A and Rozenberg M J 2011 *Nature* **469** 189
[31] Joshua A, Pecker S, Ruhman J, Altman E and Ilani S 2012 *Nat. Commun.* **3** 1129
[32] Caviglia A D, Gabay M, Gariglio S, Reyren N, Cancellieri C and Triscone J M 2010 *Phys. Rev. Lett.* **104** 126803
[33] Herranz G, Singh G, Bergeal N, Jouan A, Lesueur J, Gazquez J, Varela M, Scigaj M, Dix N, Sanchez F and Fontcuberta J 2015 *Nat. Commun.* **6** 6028
[34] Das S, Hossain Z and Budhani R C 2016 *Phys. Rev. B* **94** 115165
[35] Niu W, Zhang Y, Gan Y L, Christensen D V, Soosten M V, Garcia-Suarez E J, Riisager A, Wang X F, Xu Y B, Zhang R, Pryds N and Chen Y Z 2017 *Nano Lett.* **17** 6878
[36] Yang X, Li X M, Li Y, Li Y, Sun R, Liu J N, Bai X D, Li N, Xie Z K, Su L, Gong Z Z, Zhang X Q, He W and Cheng Z H 2021 *Nano Lett.* **21** 77
[37] Scigaj M, Gazquez J, Varela M, Fontcuberta J, Herranz G and Sanchez F 2015 *Solid State Ionics.* **281** 68
[38] Lee S W, Liu Y Q, Heo J and Gordon R G 2012 *Nano Lett* **12** 4775
[39] Lamari S 2002 *Physica E* **12** 435
[40] Vaz D C, Trier F, Dyrdal A, Johansson A, Garcia K, Barthelemy A, Mertig I, Barnas J, Fert A and Bibes M 2020 *Phys. Rev. Mater.* **4** 071001
[41] D'yakonov M I and Perel' V I 1972 *Sov. Phys. Solid State* **13** 3023